IAC-22-A6.7.10

Single-averaged models for low-thrust collision avoidance under uncertainties

Juan Luis Gonzalo[a]*, Camilla Colombo[a], Pierluigi di Lizia[a]

[a] *Department of Aerospace Science and Technology, Politecnico di Milano, Via la Masa 34, Milan, Italy 20156,* juanluis.gonzalo@polimi.it
* Corresponding Author

Abstract

This work presents a framework for the analysis of low-thrust collision avoidance activities and the design of collision avoidance manoeuvres (CAMs) under the effect of uncertainties, based on single-averaged dynamical models over the eccentric anomaly. It builds up on previous results for the tangential thrust case in the MISS (Manoeuvre Intelligence for Space Safety) software developed by Politecnico di Milano. The new models allow for the design of non-tangential manoeuvres through the superposition of analytical solutions for the tangential and normal directions. Furthermore, CAM design for probability of collision minimisation is dealt with, leveraging analytical solutions for the impulsive CAM case, and modelling the effect of uncertainties as a Gaussian distribution. A quasi-optimal, piecewise constant control profile is constructed by dividing the thrust arc into segments and assigning to each segment the thrust orientation obtained from the impulsive model. The impulsive solution, based on an eigenproblem, also provides a proxy parameter for the relative efficiency of thrusting at each segment, which can be leveraged to define the length of the thrust arc. For cases where uncertainties cannot be adequately described through a single Gaussian distribution, the use of a Gaussian Mixture Model is proposed. The performance of the models is assessed through test cases, with particular focus in analysing their range of validity depending on CAM time and total displacement. These low-thrust CAM models have applications for Space Traffic Management systems in increasingly congested scenarios and are currently being applied to a project funded by the European Space Agency for the advancement of tools for low-thrust CAM design.

Keywords: Collision avoidance manoeuvre, low-thrust, analytical methods, Space Traffic Management, Space Situational Awareness

Nomenclature

a	Semi-major axis, km
$\boldsymbol{a}_T$	Perturbing acceleration vector
a_n	Normal thrust acceleration, km/s^2
a_t	Tangential thrust acceleration, km/s^2
b	Semi-minor axis, km
e	Eccentricity
E	Eccentric anomaly, deg or rad
$\mathrm{E}[\cdot]$	Complete elliptic integral of the second kind
$\mathrm{F}[\cdot]$	Complete elliptic integral of the first kind
n	Mean motion of the spacecraft, 1/s
r	Orbital radius, km
t	Time, s
v	Orbital velocity (magnitude), km/s
$\boldsymbol{\alpha}$	Vector of Keplerian elements
Δt	Impulsive CAM lead time, s
ε	Non-dimensional thrust parameter
μ	Gravitational parameter of the primary, km^3/s^2
ω	Argument of pericentre, deg or rad
Ω	Right ascension of the ascending node, deg or rad

Acronyms/Abbreviations

CA	Close approach
CAM	Collision avoidance manoeuvre
COLA	Collision Avoidance
GMM	Gaussian mixture model
GTO	Geostationary transfer orbit
PoC	Probability of Collision
ref	Reference value
TCA	Time of closest approach

1. Introduction

The population of low-thrust-enabled spacecraft in Earth orbit is continuously growing, for a wide spectrum of missions. On the one hand, the replacement of impulsive propulsion with electric one in traditional satellites allows for extended lifetime thanks to increased propellant efficiency. On the other hand, propulsion systems manufacturers are introducing increasingly miniaturised electric thrusters that allow to provide control capabilities to small satellites that previously could not include them, even if with a very limited control authority. Together with the increase in collision avoidance (COLA) activities due to the build-up of space debris and space traffic, operators have a need for efficient models for the initial evaluation, analysis, and design of low-thrust collision avoidance manoeuvres (CAMs). These models are a foundation for parametric analyses to inform the CAM decision making process, be it operator-driven or automatised, and as first guess for more accurate numerical simulations.

A key dynamical feature of low-thrust manoeuvres in general, and CAMs in particular, is the development of clearly differentiated time scales, mainly oscillatory short-term behaviours linked to the orbital period, and a long-term evolution with characteristic period linked to thrust acceleration magnitude. This allows for highly efficient analytical and semi-analytical solutions based on perturbation methods separating both scales, for instance through averaging.

This work presents a framework for the study of low-thrust COLA activities and CAM design under the effect of uncertainties, based on single-averaged models over the eccentric anomaly. It builds up on previous results for the tangential thrust case in the MISS (Manoeuvre Intelligence for Space Safety) software developed by Politecnico di Milano [1][2]. The new models allow for the design of non-tangential manoeuvres through the superposition of analytical solutions for the tangential and normal directions. These analytical models allow for the efficient evaluation of the change in miss distance and probability of collision (PoC) due to a given CAM thrust profile, but an optimization process would still require an iterative procedure to define thrust orientation and timing, which can be computationally intensive. To address this, a procedure to define quasi-optimal, piecewise constant control profiles is proposed leveraging previous analytical solutions for the impulsive CAM [2]. The impulsive CAM model reduces the minimum PoC problem to an eigenproblem, where the optimal thrust direction is given by the eigenvector associated to the largest eigenvalue. The quasi-optimal control profile is then constructed dividing the thrust arc into segments and assigning to each segment the thrust orientation obtained from the impulsive model. The eigenvalue acts as a measure for the relative efficiency of thrusting at each segment, which can be leveraged to define the length of the thrust arc. A limitation of this approach is that the model only allows for Gaussian uncertainties. For more general cases, the use of a Gaussian Mixture Model is proposed.

These low-thrust CAM models have applications for Space Traffic Management systems in increasingly congested scenarios and are currently being applied to a project funded by the European Space Agency for the advancement of tools for low-thrust CAM design.

The rest of the manuscript is organized as follows. The COLA problem statement is given in Section 2. Section 3 presents the single-averaged used to model the effect of a CAM, for given values of the magnitude and orientation of thrust. The control law strategy is instead defined in Section 4. Uncertainty modelling is discussed in Section 5, highlighting the challenges of incorporating a GMM description into the CAM formulation. Finally, some numerical test cases are presented in Section 6, and conclusions are drawn.

2. Low-thrust COLA problem statement

Let us consider a CA between a manoeuvrable spacecraft and a debris at a time TCA. The term debris is used here in a wide sense, referring to any non-cooperative object. The spacecraft is equipped with a continuous, low-thrust propulsion system, and performs a CAM to reduce the PoC below acceptable levels. The CAM may be composed of one or several thrust arcs, followed by the corresponding coast arcs.

The low-thrust CAM is modelled using an approximate, fully analytical model as described in Section 3. The piecewise control law for the orientation and magnitude of thrust during each arc is defined from an analytical impulsive CAM solution as described in Section 4.

3. Continuous low-thrust deflection model

The low-thrust CAM is modelled following the approach in [1]. The orbit modification due to the CAM is expressed through the change of its Keplerian elements $\delta\boldsymbol{\alpha}$, where $\boldsymbol{\alpha} = [a, e, i, \Omega, \omega, M]^T$. This change is then mapped into changes in relative position and velocity at TCA using a linearized relative motion model [3]:

$$\begin{bmatrix} \delta\boldsymbol{r} \\ \delta\boldsymbol{v} \end{bmatrix}(TCA) = \begin{bmatrix} \boldsymbol{A}_r \\ \boldsymbol{A}_v \end{bmatrix} \delta\boldsymbol{\alpha}(TCA) \tag{1}$$

where $\boldsymbol{A}_r$ and $\boldsymbol{A}_v$ are 3×6 matrices that depend only on the nominal orbit [2]. Finally, the PoC and miss distance at TCA can be evaluated on the encounter plane. Note that, although we are considering only the case where the spacecraft performs a low-thrust CAM, an impulsive CAM model will also be used for the definition of the control law.

The characterization of $\delta\boldsymbol{\alpha}$ is based on Gauss's planetary equations, both for the impulsive and low-thrust cases. In general, they can be expressed as [4]:

$$\frac{\mathrm{d}\boldsymbol{\alpha}}{\mathrm{d}t} = \boldsymbol{g}(\boldsymbol{\alpha}, t; \boldsymbol{a}_T) \tag{2}$$

Function $\boldsymbol{g}$ is linear in the components of perturbing acceleration vector, so they can be rewritten in matrix form:

$$\frac{\mathrm{d}\boldsymbol{\alpha}}{\mathrm{d}t} = \boldsymbol{G}(\boldsymbol{\alpha}, t)\ \boldsymbol{a}_T \tag{3}$$

where $\boldsymbol{G}$ is a 6×3 matrix. For the impulsive CAM case, it is straightforward to obtain an expression for $\delta\boldsymbol{\alpha}$ at the time of the CAM t_{CAM} by integrating Eq. (3) over the instantaneous duration of the manoeuvre [2][5]:

$$\delta\boldsymbol{\alpha}\,(t_{CAM}) = \boldsymbol{G}_v^I(\boldsymbol{\alpha}, t_{CAM})\delta\boldsymbol{v}(t_{CAM}) \tag{4}$$

Adding a contribution to correct for the additional variation in mean anomaly due to the change in mean motion between t_{CAM} and TCA [6][2], the expression for $\delta\boldsymbol{\alpha}$ at TCA is reached:

$$\delta\boldsymbol{\alpha}\,(TCA) = \boldsymbol{G}_M^I(\boldsymbol{\alpha}, \Delta t)\delta\boldsymbol{\alpha}\,(t_{CAM}) \tag{5}$$

where $\Delta t = TCA - t_{CAM}$ is the lead time of the manoeuvre. Note that, because the mapping between $\delta\boldsymbol{\alpha}$ and displacement at CA $\delta\boldsymbol{r}$ is also linear, a linear expression is reached between the CAM $\delta\boldsymbol{v}$ and $\delta\boldsymbol{r}$. This is leveraged in Section 4 to define the quasi-optimal control law.

The development of a continuous-thrust model for $\delta\boldsymbol{\alpha}(TCA)$ is significantly more involved than for the impulsive case. A first semi-analytical solution for the tangential thrust case, which is the quasi-optimal orientation for CAM lead times larger than half an orbit, was proposed by the authors in [7]. It is based on the single-averaging of Gauss's planetary equations over the eccentric anomaly E, reaching analytic expressions for the mean evolution of the Keplerian elements in terms of complete elliptic integrals of the first and second kinds. However, considering only the mean evolution of $\delta\boldsymbol{\alpha}$ was not enough to reach a sufficient accuracy for the change of phasing at TCA, requiring the inclusion of short-periodic corrections derived through a numerical fitting. The calculation of the coefficients of the numerical fitting and the integration of the time law were performed numerically, preventing the model from being entirely analytical. This limitation was addressed in [8], obtaining analytical expressions for the short-periodic terms and the time law in the form of series expansions in the reference eccentricity. Although the expansion in e_{ref} could limit applicability for highly-eccentric orbits, numerical test cases show that the model behaves well for typical values including up to GTOs [9].

As previously mentioned, a change of independent variable from time to eccentric anomaly E is required as part of the averaging process. This is done through the definition of a differential time law:

$$\frac{\mathrm{d}t}{\mathrm{d}E} = \tau(\boldsymbol{\alpha}, t; \boldsymbol{a}_T) \tag{6}$$

In [7], an approximated time law derived from Kepler's equation was used, based on [10][11]. It was later noted in [8] that this approximate time law corresponds to neglecting acceleration in Gauss's planetary equation for E. Indeed, inverting Gauss's planetary equation for the eccentric anomaly and expanding in power series of the perturbing acceleration up to first order terms yields:

$$\begin{aligned}\frac{\mathrm{d}t}{\mathrm{d}E} = \sqrt{\frac{a^3}{\mu}}(1 - e\cos E) + \frac{1}{\mu}\tau^t(a, e, E) \\ + \frac{1}{\mu}\tau^n(a, e, E) \\ + \mathcal{O}(a_t^2, a_n^2, a_t a_n)\end{aligned} \tag{7}$$

where τ^t and τ^n are functions of the semi-major axis, eccentricity, and eccentric anomaly. It is straightforward to check that the first term of the right-hand side corresponds to the derivative of Kepler's equation with respect to E, as already indicated. As a consequence, both time laws will provide the same differential equations for $\mathrm{d}\boldsymbol{\alpha}/\mathrm{d}E$ up to first order terms in thrust acceleration. However, they will yield different results for the approximate analytic time law $E(t)$. The numerical analyses in [8][9] show that the time law including first order terms in thrust acceleration behaves better in general, and it will be the one considered in this work.

The low-thrust CAM model in [8][7] only considers acceleration in the tangential direction. Although this is the dominant component when CAM lead time is long enough [2], small contributions in the normal direction can also appear, particularly as lead time decreases below half an orbital revolution. The work by Gao [12] shows that, for small thrust magnitudes, the contributions from different control strategies can be combined linearly. This can also be observed from Eq. (3): given that the variations in $\boldsymbol{\alpha}$ due to the low-thrust actions are scaled by the thrust magnitude, the contributions from the components of $\boldsymbol{a}_T$ up to first order are decoupled. Note that the approximation of considering up to first order terms in $\boldsymbol{a}_T$ was already required for the approximate differential time law, as previously discussed. Consequently, the change in Keplerian elements due to a generic in-plane CAM thrust acceleration is expressed as:

$$\delta\boldsymbol{\alpha}(E; \varepsilon_t, \varepsilon_n) = \delta\boldsymbol{\alpha}^t(E; \varepsilon_t) + \delta\boldsymbol{\alpha}^n(E; \varepsilon_n) \tag{8}$$

where $\varepsilon_t = a_t/(\mu/a_{ref}^2)$ and $\varepsilon_n = a_n/(\mu/a_{ref}^2)$ are non-dimensional thrust parameters in the tangential and normal directions, respectively [8][9]. The detailed derivation of the expressions for $\delta\boldsymbol{\alpha}^t(E; \varepsilon_t)$ can be found in [9][8] and is omitted here for brevity. The solutions for semi-major axis and eccentricity show secular and oscillatory contributions:

$$\begin{aligned}\delta a^t &= \varepsilon_t[K_a^t E + a_{osc}^t(E)]_{E_0}^E \\ \delta e^t &= \varepsilon_t[K_e^t E + e_{osc}^t(E)]_{E_0}^E\end{aligned} \tag{9}$$

The secular terms are linear with slopes function of complete elliptic integrals of the first and second kinds:

$$
\begin{aligned}
K_a &= \frac{4a_{ref}\ \mathrm{E}\left[e_{ref}^2\right]}{\pi} \\
K_e &= \frac{4\left(1-e_{ref}^2\right)}{e_{ref}\pi}\left(\mathrm{E}\left[e_{ref}^2\right]-\mathrm{F}\left[e_{ref}^2\right]\right)
\end{aligned} \tag{10}
$$

where a_{ref} and e_{ref} are the reference semi-major axis and eccentricity, respectively, of the averaged solution. Note that these values can be obtained numerically imposing the initial conditions $a\left(E_0; a_{ref}, e_{ref}\right) = a_0$ and $e\left(E_0; a_{ref}, e_{ref}\right) = e_{ref}$.

The oscillatory terms $a_{osc}^t(E)$ and $e_{osc}^t(E)$ are expressed as power series of e_{ref}, and contain increasing harmonics of E. The full expressions are derived in [8], and reported in Appendix A for convenience. On the other hand, the solution for $\delta\omega^t$ does not show a secular evolution, and can be expressed as:

$$
\delta\omega^t = \varepsilon\frac{2\sqrt{1-e_{ref}^2}}{e_{ref}^2}\left(2\,\mathrm{asin}\sqrt{\frac{1-e_{ref}c_E}{2}} - \sqrt{1-e_{ref}^2c_E^2}\right)\Bigg|_{E_0}^{E} \tag{11}
$$

where $c_E = \cos E$. Finally, a tangential thrust action does not introduce changes in inclination and right ascension of the ascending node.

The models for $\delta\boldsymbol{\alpha}^n(E;\varepsilon_n)$ are now introduced. A first attempt at obtaining a normal-thrust solution analogous to the tangential one was carried out in [9]; however, although a solution in terms of incomplete elliptic integrals of the three kinds was reached, it was too cumbersome for practical use. In this work, a solution for the normal thrust case following the same structure as the tangential one is presented. From Eq. (2) and [4], the non-zero Gauss's planetary equations for a normal thrust acceleration are:

$$
\begin{aligned}
\frac{\mathrm{d}e^n}{\mathrm{d}t} &= -a_n\frac{r\sin f}{av} \\
\frac{\mathrm{d}\omega^n}{\mathrm{d}t} &= a_n\frac{\left(2e+\dfrac{r}{a}\cos f\right)}{ev} \\
\frac{\mathrm{d}E^n}{\mathrm{d}t} &= \frac{an}{r} - a_n\frac{r(e+\cos f)}{bev}
\end{aligned} \tag{12}
$$

Using the last of Eq. (12) to perform the change of independent variable of the differential equations for e and ω, plugging in the definition of ε_n and retaining up to first order terms in ε_n one reaches:

$$
\begin{aligned}
\frac{\mathrm{d}e^n}{\mathrm{d}E} &= -\varepsilon_n\sqrt{1-e^2}\frac{(1-e\,c_E)\,s_E}{\sqrt{\dfrac{1+e\,c_E}{1-e\,c_E}}} + \mathcal{O}(\varepsilon_n^2) \\
\frac{\mathrm{d}\omega^n}{\mathrm{d}E} &= \varepsilon_n\frac{(e+c_E)(1-e\,c_E)^2}{e\sqrt{1-e^2c_E^2}} + \mathcal{O}(\varepsilon_n^2)
\end{aligned} \tag{13}
$$

where $c_E = \cos E$ and $s_E = \sin E$. It is straightforward to integrate the equation for e:

$$
\begin{aligned}
\Delta e^n(E) &= \\
&= \frac{\varepsilon_n\sqrt{1-e_{ref}^2}}{2\,e_{ref}}\left(\left(4+e_{ref}c_E\right)\sqrt{1-e_{ref}^2c_E^2} + 6\,\mathrm{acot}\sqrt{\frac{1-e_{ref}c_E}{1+e_{ref}c_E}}\right)\Bigg|_{E_0}^{E} \\
&\quad + \mathcal{O}(\varepsilon_n^2)
\end{aligned} \tag{14}
$$

while for ω, a solution in terms of complete elliptic integrals of the first and second time can be reached through careful manipulation. Expanding in power series of the reference eccentricity of the averaged solution, e_{ref}, an expression separating a linear secular and oscillatory short-periodic components in E is reached:

$$
\omega^n(E;\varepsilon_n) = \omega_{ref} + \varepsilon_n K_\omega^n E + \varepsilon_n\omega_{osc}(E) + \mathcal{O}(\varepsilon_n^2) \tag{15}
$$

where ω_{ref} is the reference argument of pericentre of the averaged solution, that can be computed analogously to a_{ref} and e_{ref}. The slope of the secular term, K_ω^n, is a function of complete elliptic integrals of the first and second kind of e_{ref}:

$$
K_\omega^n = \frac{2\sqrt{1-e_{ref}^2}}{e_{ref}^2\pi}\left(\left(2-e_{ref}^2\right)\mathrm{E}\left[-\frac{e_{ref}^2}{1-e_{ref}^2}\right] - 2e_{ref}\mathrm{F}\left[-\frac{e_{ref}^2}{1-e_{ref}^2}\right]\right) \tag{16}
$$

The short-periodic terms are given as a series expansion on e_{ref} of the form:

$$
\omega_{osc}(E) = \sum_{u=1,2,..} e_{ref}^{u-2}\sum_{v=1}^{u} M_{uv}^{\omega}\sin vE \tag{17}
$$

where $\boldsymbol{M}^{\omega}$ is a matrix of constant coefficients. The values up to $(u, v) = (6,6)$ are reported below:

$$\boldsymbol{M}^{\omega} = \begin{bmatrix} 1 & 0 & 0 & 0 & 0 & 0 \\ 0 & -\frac{1}{2} & 0 & 0 & 0 & 0 \\ -\frac{7}{8} & 0 & \frac{1}{8} & 0 & 0 & 0 \\ 0 & \frac{1}{8} & 0 & -\frac{1}{2} & 0 & 0 \\ -\frac{13}{64} & 0 & \frac{1}{128} & 0 & \frac{7}{640} & 0 \\ 0 & \frac{11}{256} & 0 & -\frac{1}{128} & 0 & -\frac{1}{256} \end{bmatrix}$$

The time law in implicit form $t(E)$ can be obtained substituting the solutions for $\boldsymbol{\alpha}^t$ and $\boldsymbol{\alpha}^n$ into differential Eq. (7), expanding in power series of thrust magnitude up to first order terms, and integrating. Owing to the simple expressions reached for $\delta\boldsymbol{\alpha}^t$ and $\delta\boldsymbol{\alpha}^n$, this integration is straightforward to perform analytically in a symbolic manipulator. Nevertheless, it is not possible to obtain an explicit solution for the explicit form $E(t)$, so the evaluation of eccentric anomaly for a given time still requires a numerical root finding.

4. Quasi-optimal piecewise-control law

A procedure for the fast construction of a piecewise-constant, quasi-optimal CAM control profile is derived from the impulsive CAM model. In the impulsive model, following the approach proposed by Bombardelli and Hernando-Ayuso [13] it is possible to reduce the PoC minimization CAM design problem to a quadratic one with cost function:

$$J = \delta\boldsymbol{v}^{\mathrm{T}}\, \boldsymbol{Z}\, \delta\boldsymbol{v} \tag{18}$$

Matrix $\boldsymbol{Z}$ is defined leveraging Chan's formulation of PoC [14], and it depends on the matrices describing the linear dynamical model for the impulsive CAM, as well as the elements of the uncertainty covariance in the encounter plane. For the dynamical model in this work, it can be expressed as:

$$\boldsymbol{Z} = (\boldsymbol{A}_r \boldsymbol{G}_M^I \boldsymbol{G}_v^I)^T \boldsymbol{Q} (\boldsymbol{A}_r \boldsymbol{G}_M^I \boldsymbol{G}_v^I) \tag{19}$$

where $\boldsymbol{Q}$ is a matrix that depends on the components of the combined Gaussian covariance of the encounter, projected in the encounter plane [2].

The advantage of having a quadratic cost function like the one in Eq. (18) is that the optimization problem can be reduced to an eigenproblem [15]. Particularly, the optimal impulsive CAM direction is given by the eigenvector associated to the largest eigenvalue of $\boldsymbol{Z}$.

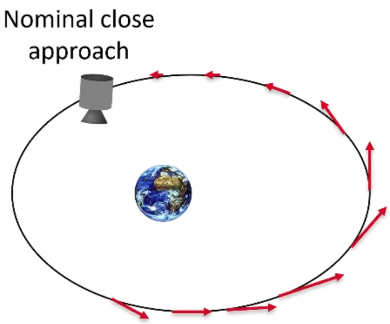

Fig. 1. Piecewise-constant control profile concept

Dividing the thrust arc in several segments and applying this model at the middle point of each segment, a piecewise-constant profile for the low-thrust CAM orientation is obtained, Fig. 1. However, Eq. (18) does not provide direct information on the magnitude of thrust. Indeed, cost function J is unbounded in the magnitude of $\delta\boldsymbol{v}$, and the minimum PoC solution corresponds to using as much thrust as available. In practice, instead, we will want to reach a pre-set PoC threshold while minimizing propellant mass. For a low-thrust case, this typically leads to bang-bang control profile with one or more maximum-thrust arcs, with coast arcs (zero thrust) in between. To approximate this behaviour, the magnitude of the largest eigenvalue of $\boldsymbol{Z}$ can be used as proxy. Recalling that the optimal CAM for minimum PoC is aligned with the eigenvector $\mathbf{ei}$ associated to the largest eigenvalue γ, and that the minimum PoC problem is unbounded in thrust magnitude, the optimal impulsive solution is:

$$\delta\boldsymbol{v}_{opt} = \delta v_{max}\mathbf{ei} \tag{20}$$

Substituting into Eq. (18) and operating the product of $\boldsymbol{Z}$ by its eigenvector yields:

$$J = \delta v_{max}^2\, \gamma \tag{21}$$

Showing that the magnitude of the cost function is scaled by the largest eigenvector. In this way, the eigenvalue at each segment is used as a proxy of the relative optimality of each thrust segment compared to the neighbouring ones, allowing to approximate the position of the boundaries between thrust and coast arcs.

5. Uncertainty modelling

The control law proposed in Section 4 is constructed over the minim PoC solution for the constant CAM. However, that model assumes Gaussian uncertainty distribution for the definition of matrix $\boldsymbol{Q}$. To deal with non-Gaussian uncertainty distributions, a GMM is used to reduce the problem to a superposition of Gaussian ones. However, this decomposition process is purely mathematical, with no link to the dynamical problem for the CAM. Consequently, the relative orientation of the covariance ellipsoids for each mixand can lead to conflicting orientations of the individual CAMs, and their weighted combination does not perform well in general. Further work is needed to define a framework that performs adequately in a general scenario.

6. Test cases

A possible limitation for the validity of the single-averaged low-thrust CAM model is the expansion in the reference eccentricity e_{ref}, needed to separate the secular and short-periodic contributions. Recall that this separation is important for computational cost reasons: although a non-expanded solution can be obtained in terms of incomplete elliptic integrals of the first and second kind, their use requires the evaluation of E[·] and F[·] for each value of the eccentric anomaly. In contrast, the separated solution only requires one evaluation for all values of E. The good behaviour of the tangential thrust solution for relatively high values of e_{ref} was already studied in [9]. Regarding the newly proposed normal thrust model, the only element requiring the expansion in the argument of pericentre.

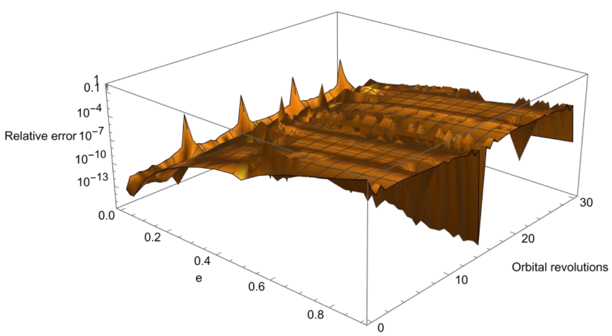

Fig. 2. Relative error for the ω^n model, normalized by thrust magnitude and for a wide range in eccentricity and manoeuvre duration

Fig. 2 shows the relative error for ω^n compared with a numerical propagation, for the model given in Eqs. (15)-(17) and 7 terms of the short-period expansion. Results are normalized by thrust magnitude. As expected, error grows with initial eccentricity, but it still performs well for values higher than a GTO. The reason can be better understood by comparing with the results obtained by expanding in power series of eccentricity before integration, shown in Fig. 3. This solution is simpler to derive, and it does not involve elliptic functions. However, it also shows a significantly degraded accuracy. It is concluded that the separation in secular and short-periodic terms after the integration allows to improve the model accuracy by restricting the series expansion only to the short-periodic terms, whose contribution is bounded and their structure changes slowly with eccentricity.

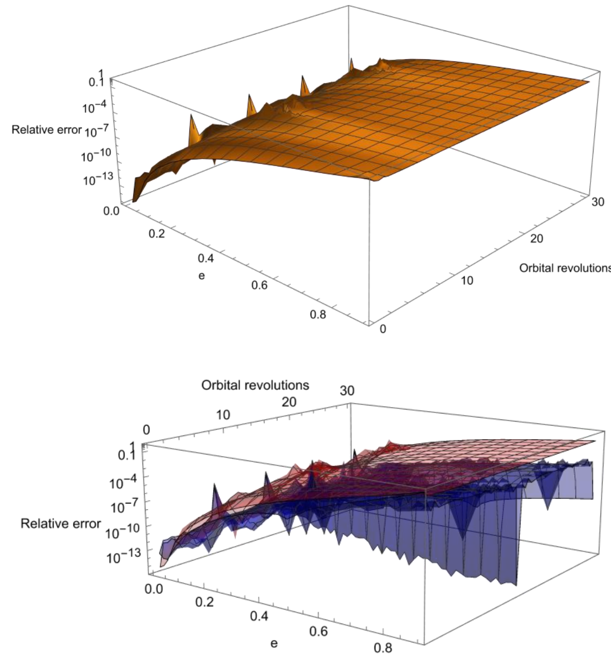

Fig. 3. Relative error for a ω^n solution obtained by fully expanding the differential equation in e before integration (top), and comparison with the secular + short-periodic solution (bottom)

7. Conclusions

An approximate analytical model for continuous, low-thrust, in-plane CAMs has been presented. This is an extension of previous results, where the model for tangential CAMs was derived. By expanding the solution in power series of the small thrust acceleration up to first-order terms, the contributions from the tangential and normal components can be decoupled, and their analytical solution treated separately. To obtain analytical expressions for the orbit change due to the CAM along each direction, the Gauss's planetary equations are averaged over one revolution in eccentric anomaly after a change of independent variable, and the results are expressed as a linear secular term (with rate of change function of complete elliptic integrals of the first and second kinds) and oscillatory short-periodic terms (expressed as a power series in the reference eccentricity). Numerical results show the good accuracy of these models for typical values of nominal orbit and thrust acceleration, making them useful for preliminary and parametric analyses.

Regarding optimal CAM design, an analytical model for impulsive CAMs is leveraged to design piecewise-constant, quasi-optimal minimum PoC manoeuvres. By dividing the thrust arcs in multiple segments, the impulsive CAM result provides both the locally optimal direction of thrust, as well as a parameter quantifying how convenient it is to thrust in said segment compared to the neighbouring ones. This approach provides computationally cheap solutions that can be used for preliminary analysis or as initial guess for more detailed numerical models. A limitation of this approach is that the impulsive CAM model requires Gaussian uncertainty distributions. More general cases could be treated with a GMM, but the direct superposition of the weighted results for each mixand does not provide good results in general. Further work to define a framework for the use of GMM in combination with the proposed CAM model is required.

Acknowledgements

This work has received funding from the European Space Agency through the project "ELECTROCAM: Assessment of collision avoidance manoeuvre planning for low-thrust missions" (call AO/1-10666/21/D/SR). It has also received funding from the European Research Council (ERC) under the European Union’s Horizon 2020 research and innovation programme (grant agreement No 679086 – COMPASS).

Appendix A

The oscillatory components for the tangential-thrust solution of semi-major axis and eccentricity take the form:

$$\begin{aligned} a_{osc}^{t}(E) &= \sum_{u=1,2,..} e_{ref}^{2u} \sum_{v=1}^{u} M_{uw}^{a} \sin 2vE \\ e_{osc}^{t}(E) &= \sum_{u=1,2,..} e_{ref}^{u-1} \sum_{v=1}^{u} M_{uw}^{e} \sin vE \end{aligned} \tag{22}$$

Note that semi-major axis only contains even harmonics in E. The coefficient matrices $\boldsymbol{M}^a$ and $\boldsymbol{M}^e$ are derived with the assistance of a symbolic manipulators, and their elements up to order 6 are (the coefficients up to order 8 can be found in [8]):

$$\boldsymbol{M}^a = a_{ref} \begin{bmatrix} -\frac{1}{4} & 0 & 0 \\ -\frac{1}{16} & -\frac{1}{128} & 0 \\ -\frac{15}{512} & -\frac{3}{512} & -\frac{1}{1536} \end{bmatrix}$$

$$\boldsymbol{M}^e = \begin{bmatrix} 2 & 0 & 0 & 0 & 0 & 0 \\ 0 & -\frac{1}{2} & 0 & 0 & 0 & 0 \\ -\frac{5}{4} & 0 & \frac{1}{12} & 0 & 0 & 0 \\ 0 & \frac{1}{4} & 0 & -\frac{1}{32} & 0 & 0 \\ -\frac{9}{32} & 0 & -\frac{1}{192} & 0 & \frac{3}{320} & 0 \\ 0 & \frac{19}{256} & 0 & -\frac{1}{256} & 0 & -\frac{1}{256} \\ -\frac{65}{512} & 0 & -\frac{5}{512} & 0 & \frac{11}{2560} & 0 \end{bmatrix}$$

References

[1] J.L. Gonzalo, C. Colombo, and P. Di Lizia, Introducing MISS, a new tool for collision avoidance analysis and design, Journal of Space Safety Engineering, 7, 3 (2020) 282–289. https://doi.org/10.1016/j.jsse.2020.07.010
[2] J.L. Gonzalo, C. Colombo, and P. Di Lizia, Analytical framework for space debris collision avoidance maneuver design, Journal of Guidance, Control and Dynamics, 44, 3 (2021) 469-487. https://doi.org/10.2514/1.G005398
[3] J. L. Junkins, and H. Schaub, Analytical mechanics of space systems. American Institute of Aeronautics and Astronautics, Reston, VA, 2009.
[4] R. H. Battin, An introduction to the mathematics and methods of Astrodynamics, AIAA Education series, AIAA, Reston, VA, 1999.
[5] J.L. Gonzalo, C. Colombo, and P. Di Lizia, Analysis and design of collision avoidance manoeuvres for passive de-orbiting missions, Astrodynamics 2018, series Advances in the Astronautical Sciences, 167 (2019) 2189-2208. AAS/AIAA Astrodynamics Specialist Conference, Snowbird, UT, 2018, 18–23 August.
[6] M. Vasile, and C. Colombo, Optimal Impact Strategies for Asteroid Deflection, Journal of Guidance, Control, and Dynamics, 31, 4 (2008) 858–872. https://doi.org/10.2514/1.33432
[7] J.L. Gonzalo, C. Colombo, and P. Di Lizia, A semi-analytical approach to low-thrust collision avoidance manoeuvre design, 70th International Astronautical Congress, Washington, D.C., USA, 2009, 21–25 October. Paper number IAC-19-A6.2.3
[8] J.L. Gonzalo, and C. Colombo, Lightweight algorithms for collision avoidance applications, 11th ESA GNC, virtual conference, 2021, 22-25 June.
[9] J.L. Gonzalo, C. Colombo, and P. Di Lizia, Computationally Efficient Approaches for Low-Thrust Collision Avoidance Activities, 72nd International Astronautical Congress, Dubai, UAE,

2021, 25-29 October. Paper number IAC-21-A6.10-B6.5.5.

[10] S. Huang, C. Colombo, and F. Bernelli-Zazzera, Orbit raising and de-orbit for coplanar satellite constellations with low-thrust propulsion, IAA-AAS-DyCoSS4-1-15, 4th IAA Conference on Dynamics and Control of Space Systems, Changsha, China, 2018, 21–23 May.

[11] S. Huang, C. Colombo, E.M. Alessi, and Z. Hou, Large constellation de-orbiting with low-thrust propulsion, AAS 19-480, 29th AAS/AIAA Space Flight Mechanics Meeting, Ka'anapali, HI, 2019, 13–17 January.

[12] Y. Gao, Near-optimal very low-thrust earth-orbit transfers and guidance schemes, Journal of Guidance Control and Dynamics, 30, 2 (2017), 529-539.

[13] C. Bombardelli, J. Hernando Ayuso, Optimal Impulsive Collision Avoidance in Low Earth Orbit, Journal of Guidance, Control, and Dynamics, 38, 2 (2015), 217-225. https://doi.org/10.2514/1.G000742

[14] F. K. Chan, Spacecraft Collision Probability, Aerospace Press, 2008, Chap. 6.

[15] B. Conway, Near-Optimal Deflection of Earth-Approaching Asteroids, Journal of Guidance, Control, and Dynamics, 24, 5 (2001), 1035–1037. https://doi.org/10.2514/2.4814